

## Introduction

**Prompt Elasto-Gravity Signals (PEGS)**, generated by large earthquakes, propagate at the speed of light and are sensitive to the earthquake magnitude and focal mechanism. These characteristics make PEGS potentially very advantageous for earthquake and tsunami early warning. PEGS-based early warning does not suffer from the saturation of magnitude estimations problem and does not require a priori assumptions on slip distribution.

We use a deep learning model called **PEGSNet**, to track the temporal evolution of the magnitude of the 2010 Maule earthquake, Mw=8.8. The model is a Convolutional Neural Network (CNN), trained on a database of synthetic PEGS, augmented with empirical noise.

Our results indicate that PEGSNet could have estimated that the magnitude of the Maule earthquake was above 8.7, 90 seconds after origin time.

## Data and PEGSNet

We compute synthetic PEGS by reconstructing the total moment tensor, for a set of subduction earthquake scenarios at the available stations in 2010 and in 2021. Location, strike and dip angles are generated following the Slab2.0 model. Magnitude and rake angles are generated following uniform and normal distributions, respectively. Each database contains 500000 synthetic earthquake signals. We add real noise to the synthetics, recorded during 11 months at each station. We do not use P-waves.

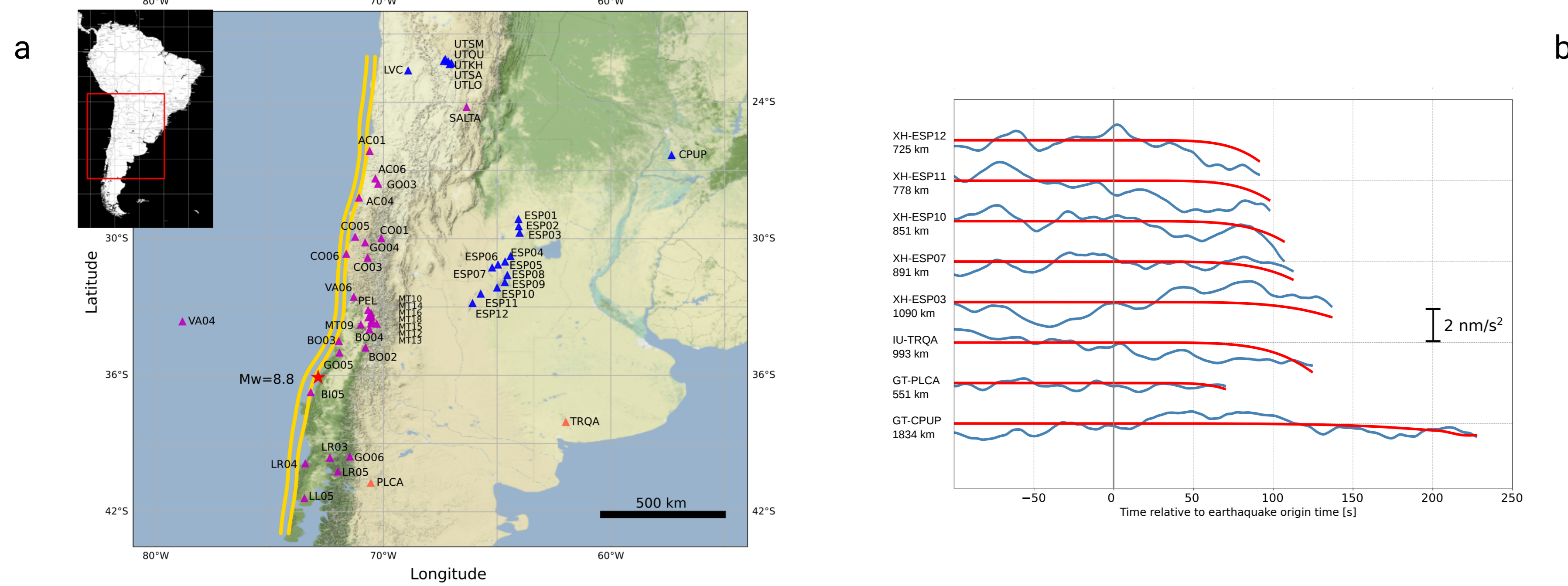


**Fig. 1** a) Setup of the two seismic networks. The yellow dots: synthetic sources location. Blue triangles: 2010 network, purple triangles: 2021 network, orange triangles: common stations. b) Some examples of the real PEGS (blue lines) recorded for the Maule earthquake vs. modeled (red lines).

PEGSNet: CNN that combines convolutional layers and fully connected layers. The model learns patterns in the data as the STF evolves with time. Labels: latitude, longitude and magnitude over time. Training, test and validation sets: 80%, 10% and 10%.

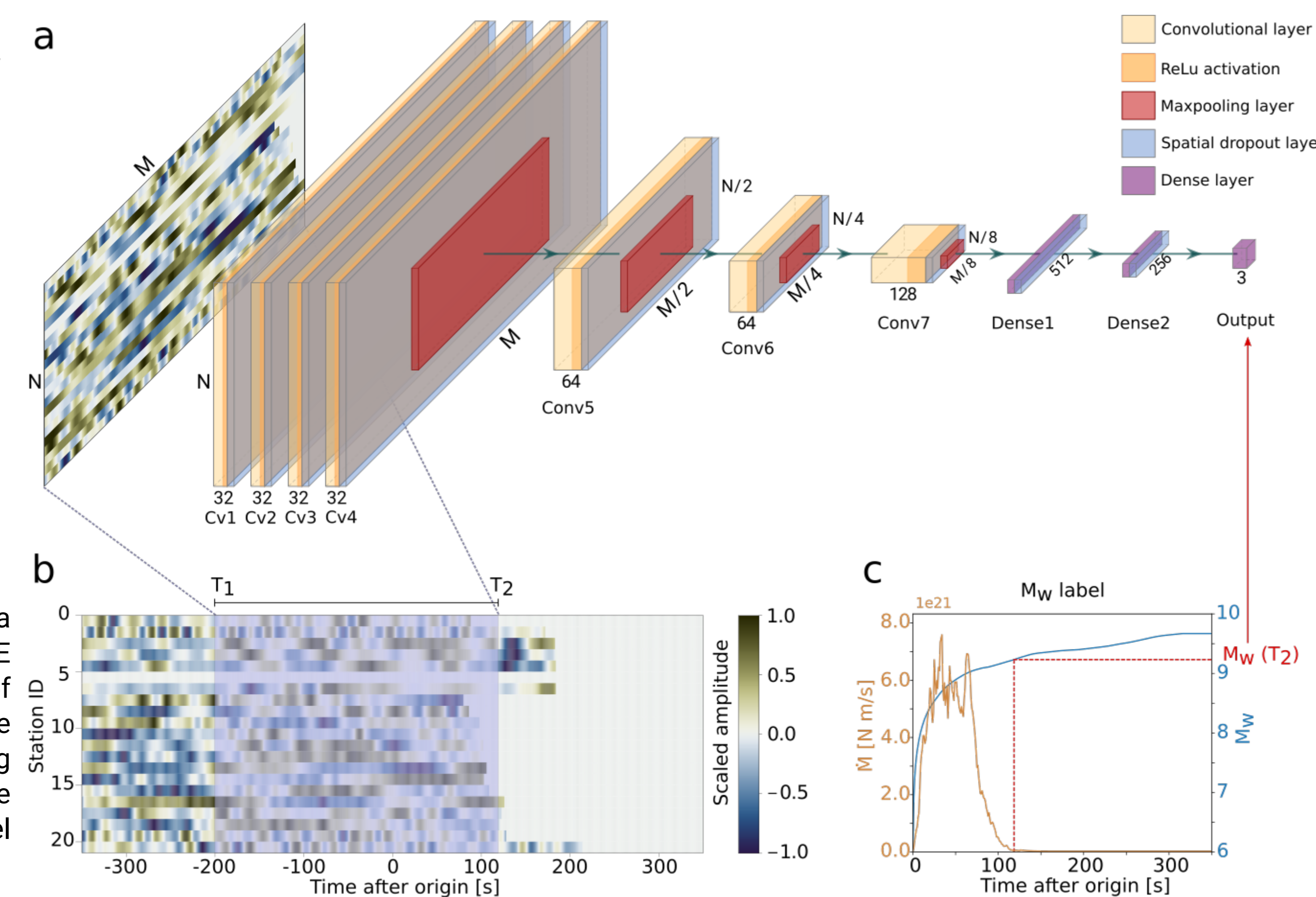


**Fig. 2** a) PEGSNet architecture: The input data are three-channel images (Z, N and E components), of shape MxN (M: number of samples, N: number of stations). b) One example of the input data from the training database (Z component). c) The blue line is the moment Mw(t) for the selected event. The label assigned is Mw(T2) at the end of the window.

## PEGSNet performance

PEGSNet can track the moment released by earthquakes with magnitude equal to or higher than 8.8, 100 s after the origin time:

2010 network: accuracy > 60%, error < 0.37

2021 network: accuracy > 55%, error < 0.46

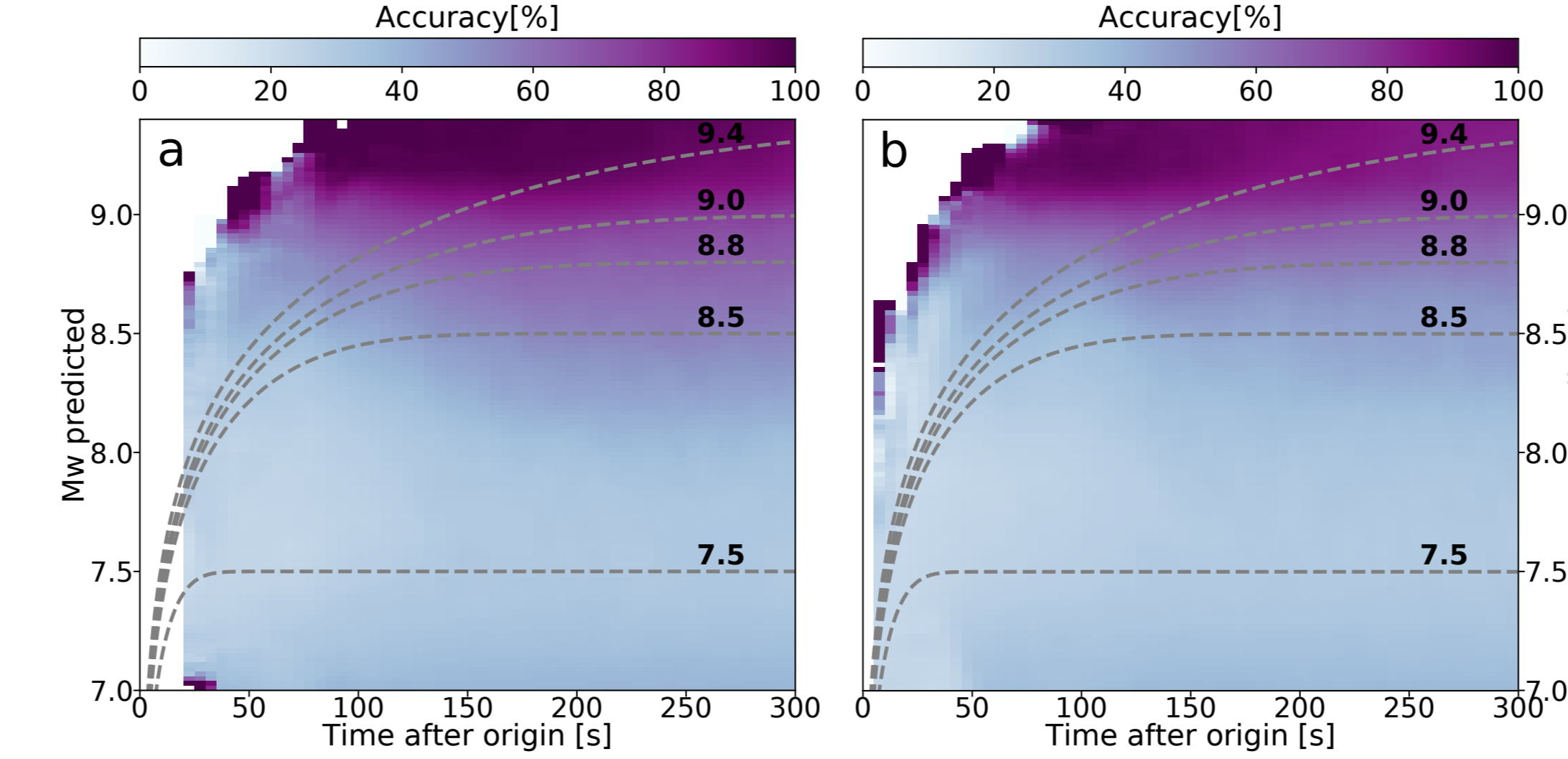


**Fig. 3** Accuracy of the predictions on the test set as a function of time and magnitude. The color at each pixel represents the number of predictions whose distance to the ground truth is less than 0.4 magnitude units, divided by the total number of samples in the bin. a and b Accuracy map for 2010 network and 2021 network.

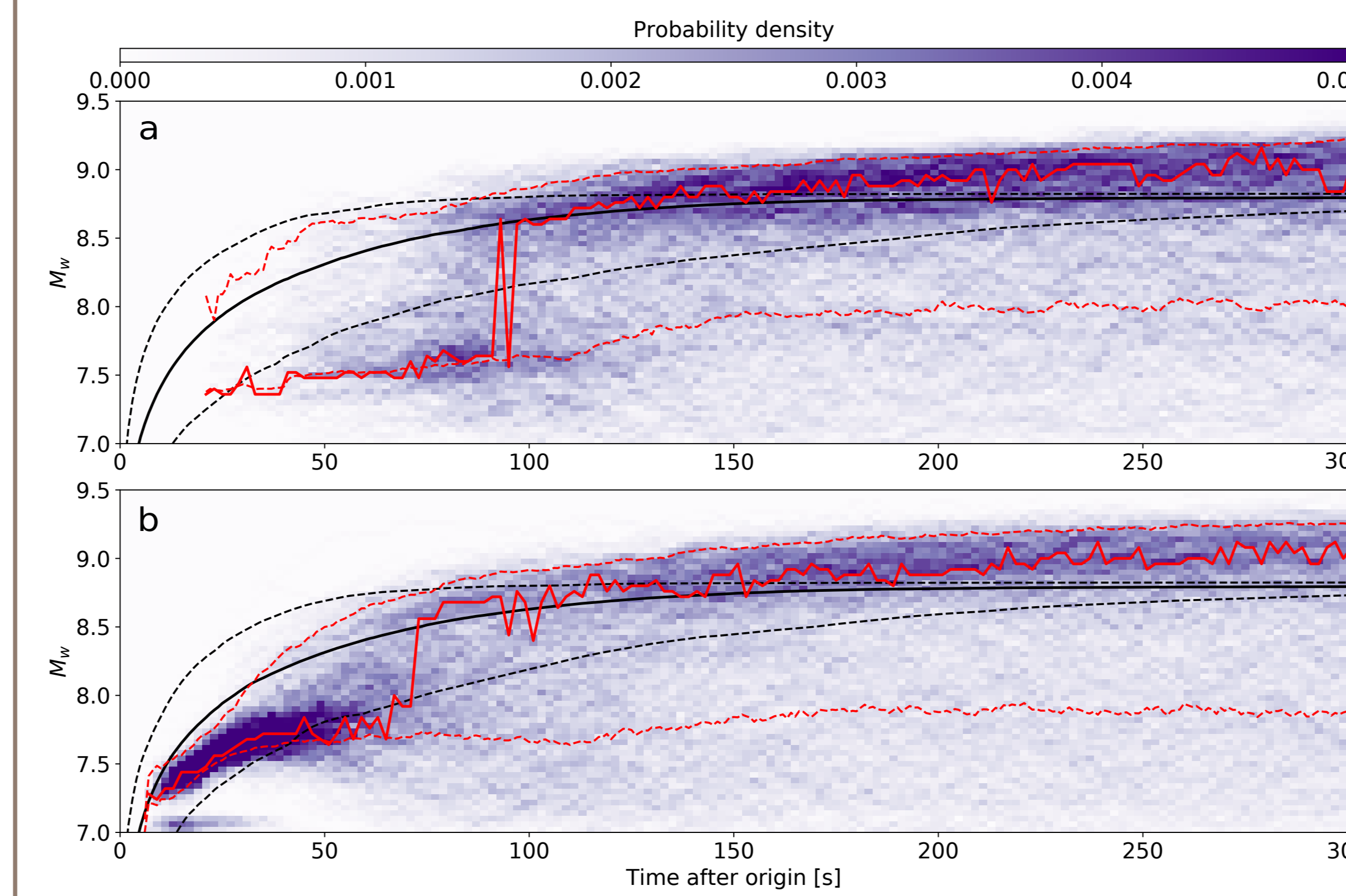


**Fig. 4** a) Probability density of the magnitude estimation (Mw 8.8 synthetic earthquakes) with the 2010 network. The solid red line is the mode of the distribution. The red dashed lines limit the range between the 95 and 25 interquartiles. The solid black line is the median of the ground truth, and the dashed black lines limit the range between the 95 and 5 interquartiles. b) Same as a for the 2021 network.

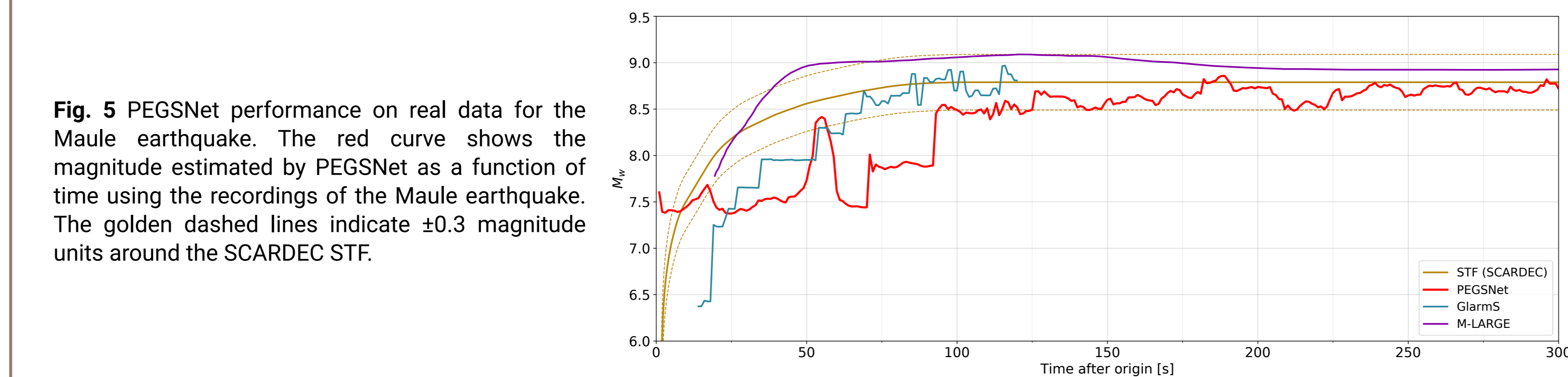
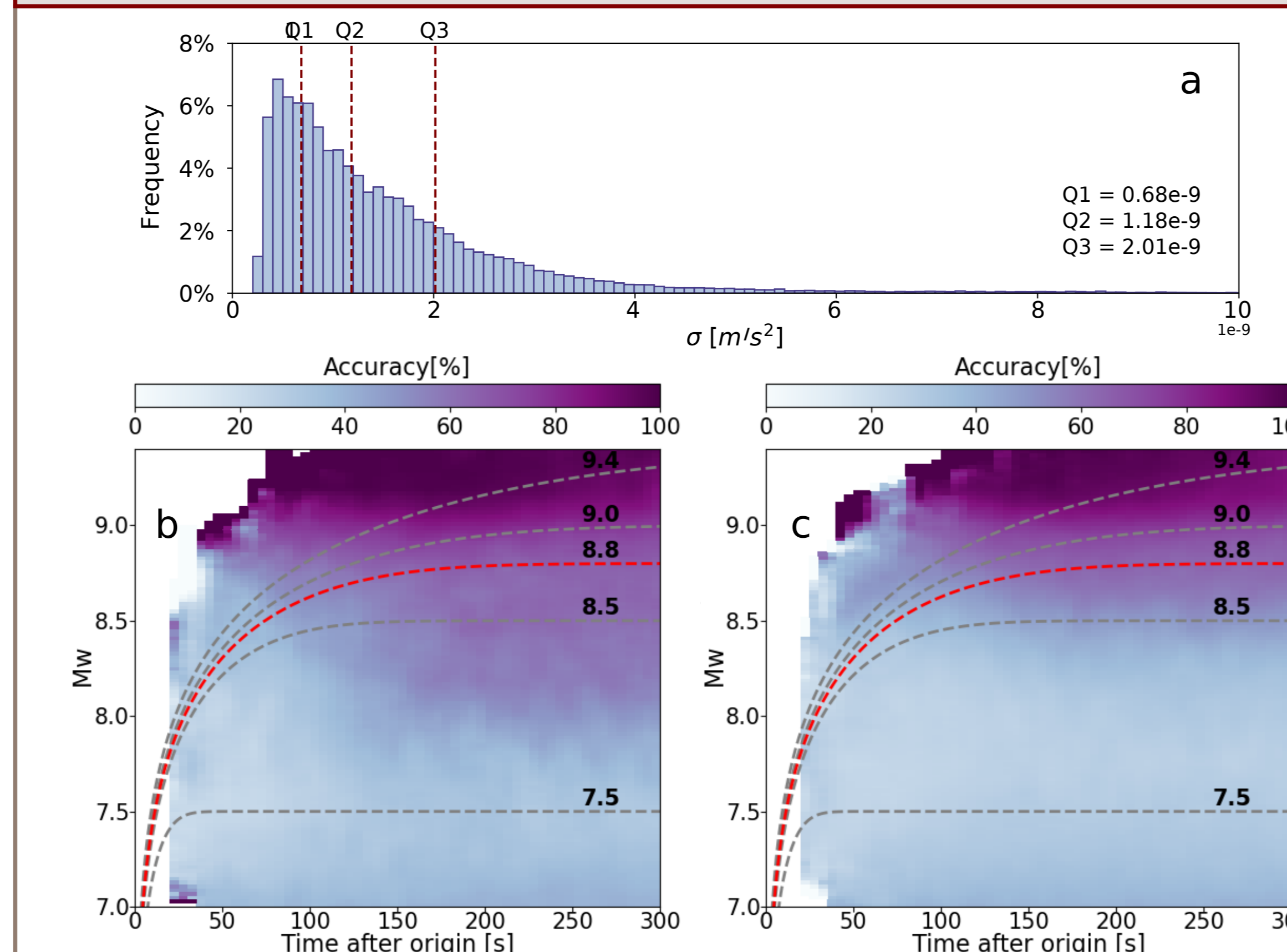


**Fig. 5** PEGSNet performance on real data for the Maule earthquake. The red curve shows the magnitude estimated by PEGSNet as a function of time using the recordings of the Maule earthquake. The golden dashed lines indicate  $\pm 0.3$  magnitude units around the SCARDEC STF.

## Noise analysis



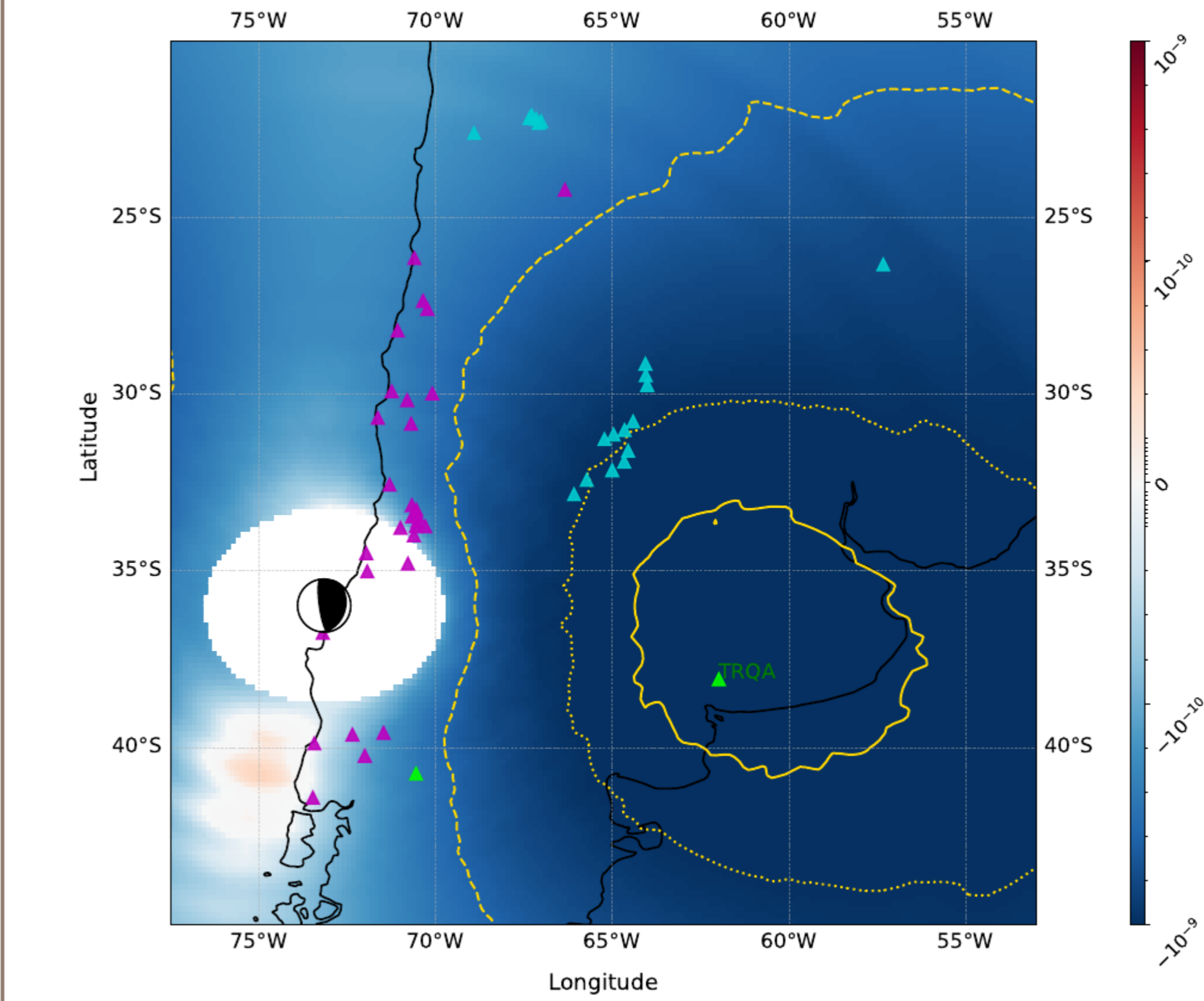
To evaluate the influence of the noise amplitude on PEGSNet's performance, we calculate the accuracy using different groups of samples of the test set, divided according to the noise level.

**Fig. 6** a) Frequency distribution of the median standard deviation of the noise ( $\sigma$ ) for the 2010 network test set. The dashed red lines indicate the first (Q1), second (Q2) and third (Q3) quartiles. The bottom panels show the accuracy maps computed using the samples for which b)  $\sigma < Q1$  and c)  $\sigma > Q3$ .

	2010 network		2021 network	
$\sigma$	Accuracy	Misfit	Accuracy	Misfit
< Q1	62 %	0.35	59 %	0.39
> Q3	59 %	0.43	51 %	0.59

**Table 1** Accuracy and misfit values calculated using the Mw  $\geq 8.8$  earthquakes 100 s after the origin time, for the 2010 and 2021 networks. Using samples with low noise level:  $\sigma < Q1$  and samples with higher noise level:  $\sigma > Q3$ .

PEGSNet performs better on 2010 network (more accuracy), even though the higher number of stations and data quality of 2021 network.



2010 network contains stations where the amplitudes of PEGS are large, while 2021 network stations are very close to the sources and the amplitudes of PEGS are small.

**Fig. 7** Spatial distribution of the maximum PEGS amplitude for the Maule earthquake, in the vertical component (at the P-wave arrival time). Turquoise triangles: 2010 network. Fuchsia triangles: 2021 network. Green triangles: common stations.

## Conclusions

The 2010 network provides delayed estimations of moment release, but higher accuracy values. The proximity of the 2021 network to the sources plays an adverse role in the model performance.

**PEGSNet is more sensitive to the geometry of the network than to the number of stations.**

The deployment of seismic stations where the larger amplitudes of PEGS are expected can improve the performance of PEGS-based early warning approaches.

## Acknowledgments

This project has received funding from the European Research Council (ERC) under the European Union's Horizon 2020 research and innovation program (Grant Agreement 949221). This work was granted access to the HPC resources of IDRIS under the allocations 2020-AD011012142, 2021-AP011012536 and 2021-A0101012314 made by GENCI. This work has been supported by the French government, through the UCAJEDI Investments in the Future project managed by the National Research Agency (ANR) ANR-15-IDEX-01.

## References

Licciardi A., Q. Bletery, B. Rouet-Leduc, J.-P. Ampuero and K. Juhel. Instantaneous tracking of earthquake growth using Prompt Elasto-Gravity Signals and Deep Learning. *Nature*, 606: 319-324 (2022)

K. Juhel, J.-P. Montagner, M. Vallée, J. P. Ampuero, M. Barsuglia, P. Bernard, E. Clévéde, J. Harms, and B. F. Whiting. Normal mode simulation of prompt elastogravity signals induced by an earthquake rupture. *Geophysical Journal International*, 216: 935-947 (2019).

Hayes, G. P. et al. Slab2, a comprehensive subduction zone geometry model. *Science*, 362(6410), 58-61 (2018).

Vallée, M., and Douet, V. A new database of source time functions (STFs) extracted from the SCARDEC method. *Physics of the Earth and Planetary Interiors*, 257: 149-157 (2016).

Pre-print here  $\rightarrow$

